ELECTRICAL/DIELECTRIC PROPERTIES OF METAL-OXIDE NANOFILMS VIA ANODIZING Al/Hf METAL LAYERS

BENDOVA Maria, MOZALEV Alexander*

CEITEC - Central European Institute of Technology, Brno University of Technology
Brno, Czech Republic, EU
*alexander.mozalev@ceitec.vutbr.cz

Abstract

Hafnium oxide (HfO_2) is a high-temperature ceramic with excellent electrical, dielectric and optical properties, which may be substantially enhanced in the nanostructured material. Here, we have developed self-organized arrays of hafnium-oxide nanorods and examined their properties by electrochemical impedance spectroscopy (EIS). For sample preparation, Al/Hf layers are magnetron sputtered onto SiO_2/Si substrates, anodized and then re-anodized to a more anodic potential. This results in the growth of a porous alumina film, followed by pore-assisted oxidation of the Hf underlayer. The films consist of discrete HfO_x protrusions, penetrating the alumina pores and anchored to a uniform oxide layer that forms under the pores. Post-anodizing treatments include annealing at 600°C in air or vacuum and selective dissolution of the alumina overlayer. The electrical/dielectric behavior of the hafnium oxide nanorod arrays, embedded in or free from alumina, was EIS-investigated in a borate buffer solution. In the re-anodized (not annealed) state the bottom oxide layer behaves as a good dielectric whereas the nanorods are semiconducting in nature. This situation does not change substantially by the annealing in air, still resulting in a dielectric bottom layer and semiconducting nanorods. However, after the annealing in vacuum, the whole film becomes an n-type semiconductor. Further investigation is in progress to understand the formation-structure-morphology relationship, aiming at exploring the functional properties of the films.

Keywords: Porous anodic alumina, anodizing, nanostructured hafnium oxide, dielectric, semiconductor

1. INTRODUCTION

Hafnium oxide (HfO_2) is a high-temperature ceramics with excellent electrical and optical properties, which makes it promising for a wide variety of relevant applications [1]. The outstanding chemical stability, large bandgap (5.5-6.0 eV), relatively high dielectric constant (22-25), high breakdown field strength (3.9-6.7 $MV \cdot cm^{-1}$), high thermal stability and large heat of formation (271 $kcal \cdot mol^{-1}$) make HfO_2 suitable in the field of electroceramics, optics, electronics, magneto-electronics, and optoelectronics [2]. HfO_2 has been identified as one of the most promising materials for the nanoelectronics industry to replace SiO_2 because of its high dielectric constant and stability in contact with Si [3].

Over the last decades, efforts have been made to enhance the properties and improve functionality of refractory ceramic films by making the films nanostructured, which is important for many applications in electronics. The growth and manipulation of HfO_2 nanocrystals and nanorods resulted in important implications for the design of optical coatings. Despite the large number of potential applications and useful properties, the well-controlled preparation of nanostructured hafnium oxide films with the reproducible chemical composition, crystal structure and nano-morphology remains a challenge. This is partly because the optical, electrical and electro-optic properties of HfO_2 are highly dependent on the surface/interface structure and chemistry [1-3].

Various deposition methods have been tried to synthesize hafnium-based nanomaterials [1-4]. They are generally divided into solution processes (sol-gel, anodizing) and gas-phase processes including both physical (sputtering, PLD) and chemical ((MO)CVD, ALD) vapor deposition methods. However, HfO_2 ceramics practically available usually present poor crystallinity, irregular particles with broad size distribution and low

surface area. Therefore, it is desirable to design and develop a facile technology for the large-scale synthesis of HfO_2 nanostructures with consideration of versatility and affordability for practical applications.

In recent years, an original approach has been developed to grow 2-D arrays of metal-oxide nanostructures (hillocks, rods, cones etc.), anchored to dielectric or conducting substrates, via smart anodizing of a valve metal bilayer comprising a thin layer of Al superimposed on a different metal [5]. Generally, the overlying aluminium is converted into nanoporous alumina, and the self-organized growth of the underlying metal oxide occurs locally beneath the alumina pores due to a series of field-assisted electrochemical and solid state reactions. Up to now, periodic arrays of metal oxide nanostructures have been successfully grown from the couples including, for example, Ti, Ta or W [6] but not yet Hf. A major difficulty with the Hf is that anodic HfO_2 films grow usually crystalline, and the transport number for Hf^{4+} in HfO_2 anodic oxide is almost zero (<0.05) [7]. These features result in undesired oxygen evolution and hinder oxide penetration into the pores.

In the present work, for the first time, nanostructured hafnium oxide films have been synthesized via anodizing sputter-deposited Al/Hf metal layers and additionally tailored by high-voltage re-anodizing, open-circuit dissolution and high-temperature annealing. The films' electrical/dielectric properties have been examined by electrochemical impedance spectroscopy (EIS) in solution.

2. EXPERIMENTAL PART

Initial samples were prepared by dc magnetron sputter-deposition of Al/Hf bilayers on oxidized Si wafers. The metals were anodized in an acid aqueous solution giving porous anodic alumina (PAA) films (**Figure 1**), as described generally in [5]. After the aluminium layer was converted into a porous anodic oxide, an array of dot-like oxide formed on the Hf layer under the alumina pores (hereafter the *anodized* sample). Following anodizing, the samples were re-anodized to a more anodic potential in a solution giving compact-type films to achieve self-directional growth of relatively long aspect ratio oxide nanorods within the pores (hereafter the *re-anodized* sample). To modify the structural and electronic properties of the films, the samples were annealed in the ambient atmosphere or in a vacuum (10^{-5} Pa) at 600 °C for 3 hours (designated as the *air-annealed* and *vacuum-annealed* samples, respectively). For comparative studies, the PAA film was dissolved away from selected samples (or their parts), so as to obtain the PAA-free films. Both the PAA-embedded and PAA-free samples were examined by field-emission scanning electron microscopy (SEM).

EIS measurements were carried out in a borate buffer (0.5 $mol \cdot dm^{-3}$ H_3BO_3 with 0.05 $mol \cdot dm^{-3}$ $Na_2B_4O_7$ aqueous solution of pH 7.4) at 23 °C, using an Autolab PGSTAT204/FRA32M potentiostat/galvanostat, coupled with an EIS module (Metrohm Autolab) and controlled by a PC using the software Autolab NOVA. The films were connected as working electrodes, by electrically contacting the metal that remains under the anodic films, and an Au electrode was used as counter electrode. The area of the films was confined by means of Teflon cells of 3 or 5 mm in diameter. EIS was measured at open circuit potential (OCP), by applying a sinusoidal perturbation of 10 to 100 mV to OCP in a frequency range from 1 MHz to 0.1 Hz. The data were analyzed by computer simulation and fitting using the software Autolab NOVA, the whole frequency range was used for fitting using an equivalent electrical circuit containing mostly one constant phase element (CPE, instead of a capacitance), from which effective capacitance was calculated. All area-related physical quantities were recalculated to the projected surface area, unless stated otherwise.

To estimate the dielectric constant (ε_r) of anodic HfO_2, a 95-nm thick anodic HfO_2 layer was prepared by compact anodizing of a sputter-deposited hafnium film to 50 V in the same electrolyte that was used for re-anodizing the Al/Hf bilayer samples, and its capacitance and thickness were measured by EIS and SEM, respectively, leading to ε_r of 22. This value, being in agreement with the literature [2], was used in further calculations of oxide thicknesses from the measured capacitances.

3. RESULTS AND DISCUSSION

3.1. Anodizing behavior and film morphology

By selecting appropriate formation electrical and electrolytic conditions, it was possible to grow not only a layer of anodic hafnium oxide beneath the PAA film but also an array of self-organized anodic oxide nanorods, having relatively high aspect ratios inside the alumina nanopores, i.e. within and above the alumina barrier layer. The morphological and size variations that arise from altering the anodizing variables at both the PAA formation and PAA-assisted hafnium oxidation stages are determined by the anodizing and re-anodizing potentials, which may vary up to 400 V without destructive fluctuations, which may occur due to the combined effects of stress generation and worsening the adhesion on physical defects in the films. The anodizing and re-anodizing behavior observed confirmed the growth of solid-state anodic oxide on the Hf metal underneath the alumina nanopores. The presence of nanosized rods passing through the alumina film in the re-anodized sample is directly seen in SEM images of **Figure 1**, where the sample is shown in a 3-D configuration before and after selectively dissolving the PAA layer.

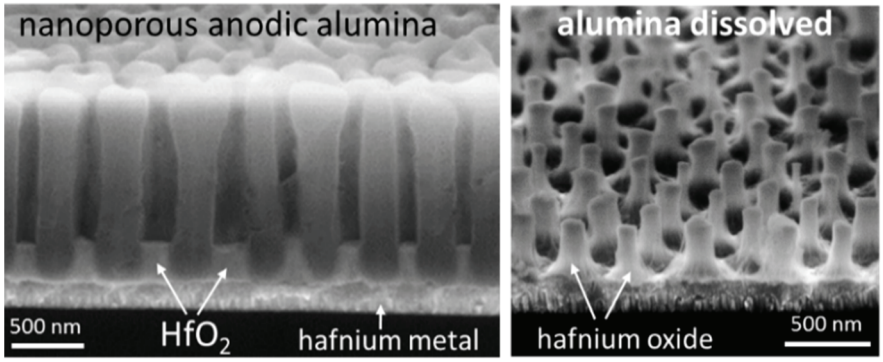

Figure 1 SEMs of an array of HfO_2 nanostructures via anodizing/re-anodizing of an Al/Hf bilayer on a SiO_2/Si substrate (a) before and (b) after selective dissolution of the PAA overlayer

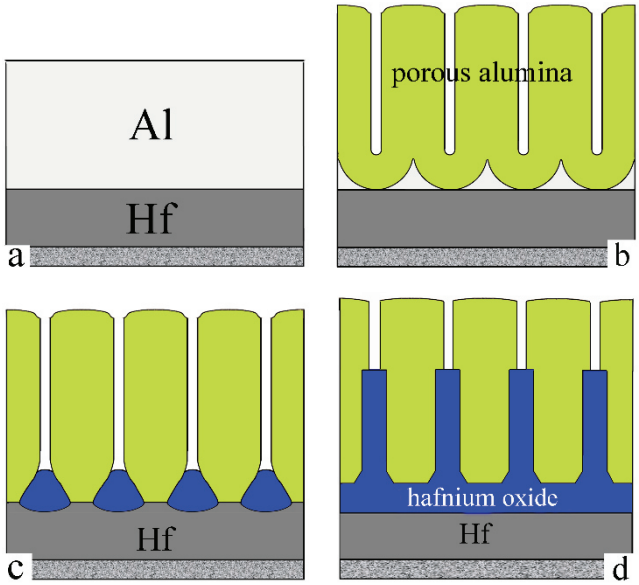

Figure 2 Schematic process for forming nanostructured HfO_2: (a) sputter-deposition of an Al/Hf bilayer onto a SiO_2-coated Si wafer, (b) anodizing of the Al layer to form a PAA film, (c) anodizing of the Hf underlayer through the PAA film (the anodized sample), (d) re-anodizing of the Hf layer to grow PAA-assisted HfO_2 nanorods (the re-anodized sample)

Based on the SEM observation, a schematic process for forming an array of HfO_2 nanorods was developed, as shown in **Figure 2**. A major feature of the anodic films formed in this way is that the hafnium-oxide nanorods are anchored to a lower layer of hafnium anodic oxide that forms under the bottom parts of the alumina barrier layer (hereafter the *bottom layer*), thus buffering the rods from the remaining hafnium substrate. Therefore, one of the objectives was to reveal the electrical properties of both parts of the films, i.e. the bottom layer and the nanorods themselves, as the first step towards functionalization of the PAA-assisted HfO_2 nanofilms.

3.2. Electrical/dielectric properties

The *re-anodized* PAA-embedded films, consisting of a bottom HfO_x layer of 90-100 nm thickness and of HfO_x nanorods ~400 nm long surrounded by the PAA matrix, reveal the capacitance of 0.20 $\mu F \cdot cm^{-2}$ and a behavior typical for a dielectric (**Figure 3a**) with a potential-independent capacitance (not shown).

After selectively etching the PAA away (PAA-free film), a very similar impedance behavior is observed, leading to only a slightly higher capacitance of 0.22 $\mu F \cdot cm^{-2}$ (**Figure 3a**), being also potential-independent (not shown). Based on the cross-sectional SEM images, the capacitance of the PAA-free film should be equal to the capacitance of the bottom oxide layer whereas the nanorods are expected to be short-circuited by the electrolyte. Thus, the thickness of the bottom oxide calculated from the measured capacitance of the PAA-free film is 90 nm, which is in a good agreement with the SEM results, and the layer is dielectric in nature. On the other hand, for the PAA-embedded film, the contribution of the nanorod-PAA layer to the total impedance, if the nanorods are also dielectric, is expected to be much higher than it was measured. With the calculated capacitance of ~0.027 $\mu F \cdot cm^{-2}$ for 400 nm long dielectric HfO_x nanorods in PAA, an overall capacitance of the PAA-embedded film of 0.024 $\mu F \cdot cm^{-2}$ is expected. This value is much lower than the measured one. Therefore, the nanorods are not dielectric but semiconducting in nature. In such a case, only a thin depletion layer forms on top of the nanorods at the interface with the electrolyte, and only the impedance/capacitance of this layer is seen by EIS, in addition to the capacitance of the bottom oxide. The measured capacitances are summarized in **Table 1**.

Table 1 The calculated capacitances of the samples prepared via PAA-assisted anodization of Hf layer

Film	Capacitance ($\mu F \cdot cm^{-2}$)	
	PAA-embedded	PAA-free
Anodized	0.32	-
Re-anodized	0.20	0.22
Air-annealed	0.110	0.115
Vacuum-annealed	40	70

In order to get a deeper insight into the semiconducting nature of the re-anodized nanorods, we also examined the *anodized* film (**Figure 3b**) The PAA-embedded anodized film showed a capacitance of 0.32 $\mu F \cdot cm^{-2}$ (**Figure 3b**), being only a little higher than one of the re-anodized film, but still no potential dependence of the capacitance is observed (not shown). Thus, the HfO_x composing the anodized film seems to be dielectric as well. The measured capacitance corresponds to an oxide thickness of 61 nm, which is in good agreement with the thickness of the bottom oxide obtained by cross-sectional SEM (~70 nm). Thus, similarly to the re-anodized film, the oxide material protruding the alumina barrier layer of ~170 nm height is rather semiconducting, whereas the bottom oxide is again dielectric.

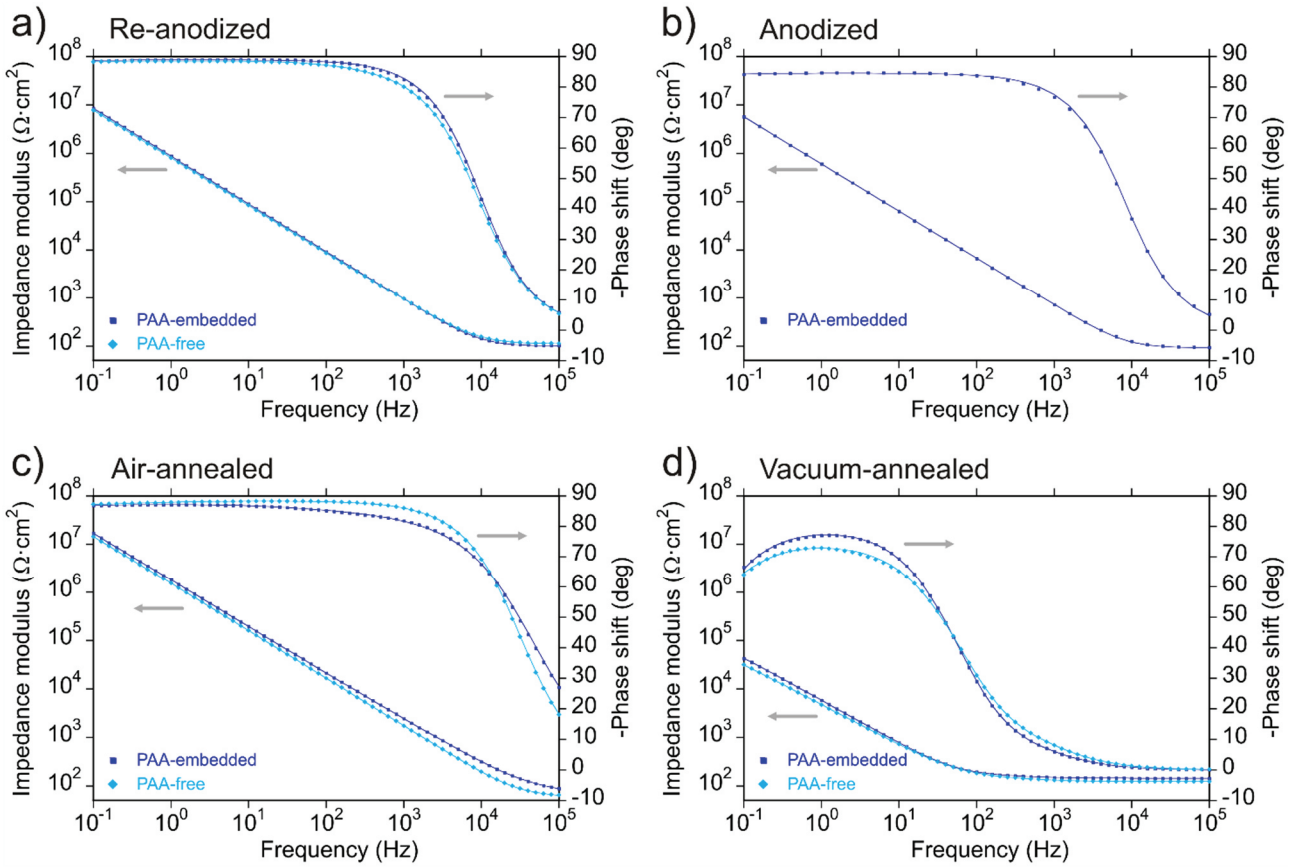

Figure 3 Bode plots obtained at OCP for the four film types in the PAA-embedded and PAA-free states: the (a) re-anodized, (b) anodized, (c) air-annealed, and (d) vacuum-annealed films. The symbols represent the measured data and the lines are the fits

The EIS behavior of the *air-annealed* films both the PAA-embedded and PAA-free (**Figure 3c**) appear to be similar to the behavior of the re-anodized films (**Figure 3a**): (1) for both the PAA-embedded and PAA-free states, a dielectric behavior is observed manifested by the potential-independent capacitance (not shown) and by phase shift approaching −90°, (2) the capacitance obtained for both states is almost the same, 0.110 and 0.115 $\mu F \cdot cm^{-2}$, respectively. The capacitance of the PAA-free film corresponds to the bottom oxide thickness of 169 nm, which is in a good agreement with the thickness estimated by SEM (~200 nm). Therefore, the air-annealed film, similarly to the re-anodized film, consists of a dielectric bottom oxide supporting rather semiconducting nanorods.

The *vacuum-annealed* films reveal a semiconducting nature of both the bottom oxide and nanorods. This is manifested by the low measured impedance and thus the high calculated capacitance and a relatively low phase shift (**Figure 3d**), as only a thin depletion layer is seen by EIS, and by a potential-dependent capacitance corresponding to an n-type semiconductor (not shown), for both the PAA-embedded and PAA-free films. The capacitances obtained at OCP are about 40 and 70 $\mu F \cdot cm^{-2}$, whereas they correspond to depletion layer thicknesses of 0.15 and 0.8 nm if an effective surface area of 30 and 300% of the projected area is taken, respectively. Such different depletion layer thicknesses would be obtained if the nanorods would have a gradient of oxygen vacancies along them, with a higher concentration at the rod tops (i.e. a thinner depletion layer) and a lower concentration at the rod bottoms (i.e. a thicker depletion layer). More analyses are needed to fully understand the behavior.

The observed peculiar electrical behavior of the PAA-assisted anodic films of HfO_x in their anodized, re-anodized, and annealed states can be explained based on the EIS characterization only with some degree of

certainty. Further insight is expected from other analyses being in progress, such as X-ray diffraction, X-ray photoelectron spectroscopy, and transmission electron microscopy combined with EDX analysis, the results to be reported in due course.

CONCLUSIONS

The main revelation from the EIS results is that the anodized, re-anodized and even air-annealed PAA-assisted hafnium oxide films have a common extraordinary feature - the bottom oxide is dielectric while the material of the nanorods behaves like a semiconductor. This feature may be beneficial for such applications like high-voltage high-value electrolytic capacitors. On the other hand, more applications, like chemical sensors, may require a fully semiconducting film, which is the case of the vacuum-annealed samples. Alternatively, the film may become fully dielectric should the right formation-annealing conditions are provided, which may extend potential applications to low-value thin-film capacitors, resistive switching devices and nanoelectronics.

ACKNOWLEDGEMENTS

Research leading to these results was supported by GAČR grant no. 17-13732S.

REFERENCES

[1] ROBERTSON, J. High dielectric constant oxides. *The European Physical Journal Applied Physics*, 2004, vol. 28, pp. 265-291.

[2] CHOI, J. H., MAO, Y., CHANG, J. P. Development of hafnium based high-*k* materials-A review. *Materials Science and Engineering: R: Reports*, 2011, vol. 72, pp. 97-136.

[3] HONG, X., ZOU, K., DASILVA, A. M., AHN, C. H., ZHU, J. Integrating functional oxides with graphene. *Solid State Communications*, 2012, vol. 152, pp. 1365-1374.

[4] RAMANA, C. V., VARGAS, M., LOPEZ, G. A., NOOR-A-ALAM, M., HERNANDEZ, M. J., RUBIO, E. J. Effect of oxygen/argon gas ratio on the structure and optical properties of sputter-deposited nanocrystalline HfO_2 thin films. *Ceramics International*, 2015, vol. 41, pp. 6187-6193.

[5] MOZALEV, A., BENDOVA, M., GISPERT-GUIRADO, F., PYTLICEK, Z., LLOBET, E. Metal-substrate-supported tungsten-oxide nanoarrays via porous-alumina-assisted anodization: from nanocolumns to nanocapsules and nanotubes. *Journal of Materials Chemistry A*, 2016, vol. 4, pp. 8219-8232.

[6] MOZALEV, A., SAKAIRI, M., TAKAHASHI, H., HABAZAKI, H., HUBALEK, J. Nanostructured anodic-alumina-based dielectrics for high-frequency integral capacitors. *Thin Solid Films*, 2014, vol. 550, pp. 486-494.

[7] PRINGLE, J. P. S. The anodic oxidation of superimposed metallic layers: Theory. *Electrochimica Acta*, 1980, vol. 25, pp. 1423-1437.